

Malaysian Journal of Mathematical Sciences

Journal homepage: https://mjms.upm.edu.my



Modified Atangana-Baleanu-Caputo Derivative for Nonlinear Thermal Wave Diffusion in Rigid Conductors: Numerical Approach

Sweilam, N. H.* ¹0¹, Bahaa El Din, N. ¹0², Ammar, M. K. ¹0², and Abo El-Dahab, E. M. ¹0²

¹Department of Mathematics, Faculty of Science, Cairo University, Giza, Egypt. ²Department of Mathematics, Faculty of Science, Helwan University, Helwan, Egypt.

E-mail: nsweilam@sci.cu.edu.eg

Received: 6 March 2025 Accepted: 25 April 2025

Abstract

This paper presents a numerical technique based on finite difference method to study numerically the behavior of a rigid thermal conductor's time-nonlinear couple system of heat wave propagation model of fractional order, where the fractional derivative is treated in the sense of Atangana-Baleanu-Caputo. It has been demonstrated via Fourier analysis that suggested scheme is unconditionally stable. Numerical experiments have been demonstrated to embed and verify the theoretical outcomes provided in this study and guarantee the effectiveness of the numerical method.

Keywords: modified Atangana-Baleanu-Caputo (MABC) fractional derivatives; propagation of time-nonlinear heat waves; stiff thermal conductor; finite difference method; stability analysis; error estimates.

1 Introduction

Nano-scale heat transport problems require advanced mathematical models due to their non-linear behavior and memory-dependent properties. Khalouta and Kadem [15] proposed a new combined method for solving nonlinear time-fractional reaction-diffusion-convection equations using Liouville-Caputo and Caputo-Fabrizio derivatives, contributing a robust tool for modeling thermal processes with memory. Similarly, Moghadam et al. [20] introduced a numerical solution for space-time variable fractional-order advection-dispersion equations via the Jacobi spectral collocation method, offering high accuracy for complex transport problems. More focus has been given recently to the nonlinear equations governing the propagation of heat waves. Ghaleb et al. [1] presented a nonlinear thermo-electroelasticity model in extended thermodynamics, forming a theoretical basis for nonlinear coupling between temperature and electric fields.

Christov and Jordan [7] analyzed second-sound propagation in nonlinear media, validating the concept of heat transfer with finite speed in such systems. Escolano et al. [10] provided analytical and numerical solutions to bidimensional lagging heat conduction models, which support the computational design of our model. Sweilam et al. [12] introduced a numerical scheme for solving space-time variable order nonlinear fractional wave equations, offering numerical techniques that guided the approach taken in this work. Jordan [13] emphasized nonlinear behavior in second-sound heat conduction in rigid materials, aligning with the assumptions made in our system. Rogolino et al. [23] contributed generalized heat transport equations incorporating both parabolic and hyperbolic models, relevant to the structure of our governing equations. Racke [22] demonstrated exponential stability in nonlinear thermoelasticity, supporting the stability section of our scheme.

Saghatchi and Ghazanfarian [24] developed SPH-based numerical methods for nanoscale heat transport, analogous to our fractional model in terms of micro-scale precision. Messaoudi and Said-Houari [19] explored blow-up phenomena in nonlinear thermoelasticity with positive energy, highlighting the criticality of energy conditions, which we consider in our boundary settings. Julius et al. [14] addressed dual-phase-lag models in heterogeneous materials, reinforcing our use of fractional-order time derivatives. Mishra [11] applied Vedic mathematics to numerical solutions, aligning with our structured discretization framework. Fractional Calculus (FC) and Fractional Differential Equations (FDEs) are widely used to describe complex systems with memory effects. Atangana and Baleanu [4] introduced a fractional derivative with a non-local and non-singular kernel, which laid the groundwork for the Atangana-Baleanu-Caputo (ABC) derivative adopted here. Maayah et al. [17] applied the ABC derivative to cancer-immune modeling, emphasizing the versatility of the operator. Reetika et al. [6] proposed a novel finite difference method for MABC derivatives, which is the core of our numerical approach.

Caputo and Fabrizio [5] introduced another fractional derivative (Caputo-Fabrizio) to handle singularity-free kernels, highlighting the evolution of fractional derivative theory. Abu Arqub et al. [2] adapted kernel-based methods with ABC distributed—order derivatives in solving fuzzy integral equations, showing broad applications in engineering models. Djennadi et al. [9] addressed the inverse time-fractional heat problem under the ABC definition, which shares features with our initial-boundary value formulation. Liu et al. [16] proposed meshless kernel-based methods for large-scale heat conduction, indicating scalability benefits relevant to our simulations. Sau et al. [25] established finite-time passivity in nonlinear systems with ABC derivatives, supporting our model's stability claims. Refai and Baleanu [3] extended the ABC derivative operator using Mittag-Leffler kernels, which we incorporate in the MABC form used here.

This work aims to study the second sound velocity dependence on heat flux and tempera-

ture and to illustrate propagation of heat waves in a stiff thermal conductor slab for nonlinear one-dimensional equations with MABC. Furthermore, we demonstrate a finite difference method along with a stability analysis for solving the proposed problem. The paper is organized as follows: Some basic definitions of fractional derivatives are given in Section 2. Section 3 describes the suggested model in terms of the MABC fractional derivative. The numerical scheme of the proposed model is derived in Section 4. Section 5 demonstrates that the obtained numerical scheme is unconditionally stable and the truncation error produced in Section 6. In Section 7, numerical results are given to show the applicability of the numerical scheme for solving the proposed model. Section 8 presents the conclusions and future work.

2 Preliminaries and Notation

This part serves as a reminder of some key fractional calculus definitions that are utilized in this paper's remaining sections.

Definition 2.1 (Riemann-Liouville Fractional Derivative). *For a function* f, *the Riemann-Liouville fractional derivative of order* $\alpha \in \mathbb{R}$ *is defined as,*

$${}_{0}D_{t}^{\alpha}f(t) = \frac{1}{\Gamma(r-\alpha)}\frac{d^{r}}{dt^{r}}\int_{0}^{t}(t-s)^{r-\alpha-1}f(s)ds, \quad t>0,$$
(1)

where r is a positive integer satisfying $r - 1 < \alpha < r$.

Definition 2.2 (Caputo Fractional Derivative). *For a function* f, *the Caputo fractional derivative of order* $\alpha \in \mathbb{R}$ *is defined as,*

$${}_{0}^{C}D_{t}^{\alpha}f(t) = \frac{1}{\Gamma(r-\alpha)} \int_{0}^{t} (t-s)^{r-\alpha-1} f^{(r)}(s) ds, \quad t > 0,$$
 (2)

where r is a positive integer satisfying $r - 1 \le \alpha < r$.

Definition 2.3 (Atangana-Baleanu-Caputo (ABC) Derivative). For $f \in H^1(0,1)$, the ABC derivative of order $0 < \alpha < 1$ is,

$${}_{0}^{ABC}D_{t}^{\alpha}f(t) = \frac{W(\alpha)}{(1-\alpha)} \int_{0}^{t} f'(s)E_{\alpha,1} \left[\frac{-\alpha}{1-\alpha} (t-s)^{\alpha} \right] ds, \tag{3}$$

with normalization function:

$$W(\alpha) = 1 - \alpha + \frac{\alpha}{\Gamma(\alpha)}, \quad W(0) = W(1) = 1, \tag{4}$$

and Mittag-Leffler function:

$$E_{\alpha,\beta}(z) = \sum_{r=0}^{\infty} \frac{z^r}{\Gamma(\alpha r + \beta)}.$$
 (5)

Definition 2.4 (Modified ABC (MABC) Derivative). For $f \in L^1(0,1)$, the MABC derivative in Caputo sense of order $0 < \alpha < 1$ is,

$${}_{0}^{MABC}D_{t}^{\alpha}f(t) = \frac{W(\alpha)}{(1-\alpha)} \left[f(t) - E_{\alpha}(-\mu_{\alpha}t^{\alpha})f(0) - \mu_{\alpha} \int_{0}^{t} (t-s)^{\alpha-1} E_{\alpha,\alpha}[-\mu_{\alpha}(t-s)^{\alpha}]f(s)ds \right], \tag{6}$$

where
$$\mu_{\alpha} = \frac{\alpha}{1-\alpha}$$
.

Remark 2.1. Fractional derivatives are powerful tools for modeling memory effects in complex processes. The MABC derivative, with its integrable singular kernel at the origin, particularly excels at describing intricate dynamical processes and enables novel solutions to certain fractional differential equations [3].

Theorem 2.1 (Stability of ABC Derivative). *The Atangana-Baleanu-Caputo derivative exhibits stable behavior under the conditions discussed in* [21] *and* [25].

3 The MABC Derivative for the Heat-Wave Equations

From a one-dimensional restriction and the purely thermodynamics formulation of a thermoelectroelasticity model as given in [1], the proposed system evolved, with an extension allowing explicit proof of how temperature and heat flux affect second sound. These equations, which describe the evolution of temperature and heat flow without assuming linearity, illustrate the effects of nonlinearity. Many evolution equations studied in the literature are linear [18].

Evolution equations are initially expressed in material coordinates. Accordingly, fractional time derivatives which arise are overall time derivatives. This leads to nonlinear evolution equations for heat flow and temperature. It is widely recognized that nonlinear systems of partial differential equations are an area of interest for continuous research in mathematical physics. In the literature, there are no exact solutions for such systems. To understand how the solutions to complex systems behave, it is crucial to use numerical and approximation methods.

The propagation of heat wave in a rigid thermal conductor slab is explained by fractional time nonlinear initial-boundary-value problem,

$$(1+\theta) \int_{0}^{MABC} D_{t}^{\alpha} \theta_{t} = -\xi_{1} (Q_{x} - QQ_{x} - \xi Q^{2}), \tag{7}$$

$$[1 + (1 + \mu_1)\theta + \mu_2 Q] \int_0^{MABC} D_t^{\alpha} Q_t = -\frac{1}{\xi_1} (\xi Q + \theta_x + \xi_2 \theta \theta_x + \xi_3 Q \theta_x), \tag{8}$$

under initial and boundary conditions:

$$\theta(0,t) = \begin{cases} \theta_0(1-\cos t), & 0 \le t \le T, \\ 0, & t > T. \end{cases}$$

$$(9)$$

$$Q(0,t) = \begin{cases} Q_0(1-\cos t), & 0 \le t \le T, \\ 0, & t > T. \end{cases}$$
 (10)

The authors in [18] provided a formula for the breaking distance and demonstrated how a given boundary-value problem can lead to blow-up of solutions.

4 Numerical Scheme Formulation Using the MABC Derivative

Starting with an equidistant mesh $t_n = n\tau$, $n = 0, 1, 2, \ldots, N$ and $x_m = mx$, $m = 0, 1, 2, \ldots, M$, we descretize (7) and (8) with step size h = L/M in the directions of space and time. The size of temporal domain segments [0,T] as well as the spatial domain [0,L] are N,M and $\tau = T/N$ respectively.

The symbols θ_n^m and Q_n^m represent approximation solution of θ and Q. Using the central difference scheme, the approximation of $(\theta_x)_n^m$ and $(Q_x)_n^m$ is given by,

$$(\theta_x)_n^m = \frac{(\theta)_n^{m+1} - (\theta)_n^{m-1}}{2h} + O(h^2), \tag{11}$$

$$(Q_x)_n^m = \frac{(Q)_n^{m+1} - (Q)_n^{m-1}}{2h} + O(h^2).$$
(12)

According to the authors in [6], the approximation of the fractional derivative in the sense of MABC is,

$$\binom{MABC}{0}D_t^{\alpha}\theta_t)_n^m = \frac{W(\alpha)}{1-\alpha} \left[\theta_n^m - E_{\alpha}(-\mu_{\alpha}t_n^{\alpha})\theta_m^0\right] - \sum_{k=0}^{n-1} \left[A_k^n \theta_{k-1}^m + B_k^n \theta_k^m + C_k^n \theta_{k+1}^m\right] + O(\tau^4),$$
(13)

$$\binom{MABC}{0}D_t^{\alpha}Q_t^{m} = \frac{W(\alpha)}{1-\alpha} \left[Q_n^m - E_{\alpha}(-\mu_{\alpha}t_n^{\alpha})Q_0^m \right] - \sum_{k=0}^{n-1} \left[A_k^n Q_{k-1}^m + B_k^n Q_k^m + C_k^n Q_{k+1}^m \right] + O(\tau^4), \tag{14}$$

where

$$\begin{split} A_k^n &= -\frac{W(\alpha)}{1-\alpha} \frac{\mu_\alpha \tau^\alpha}{2} \left[-(n-k-1)^\alpha \ _1 E_{k+1}^n - (n-k-1)^{\alpha+1} \ _2 E_{k+1}^n + (n-k)^{\alpha+1} \ _2 E_k^n \right], \\ B_k^n &= -\frac{W(\alpha)}{1-\alpha} \mu_\alpha \tau^\alpha \left[-(n-k)^\alpha \ _1 E_k^n - (n-k-1)^\alpha \ _1 E_{k+1}^n \right], \\ C_k^n &= -A_k^n, \end{split}$$

if we consider that,

$${}_{1}E_{k}^{n} = E_{\alpha,\alpha+1}(-\mu_{\alpha}(t_{n} - t_{k})^{\alpha}),$$

$${}_{2}E_{k}^{n} = E_{\alpha,\alpha+2}(-\mu_{\alpha}(t_{n} - t_{k})^{\alpha}),$$

$${}_{1}E_{k+1}^{n} = E_{\alpha,\alpha+1}(-\mu_{\alpha}(t_{n} - t_{k+1})^{\alpha}),$$

$${}_{2}E_{k+1}^{n} = E_{\alpha,\alpha+2}(-\mu_{\alpha}(t_{n} - t_{k+1})^{\alpha}).$$

Substituting (11)–(14) into (7) and (8), we obtain,

$$(1+\theta_{n}^{m})\frac{W(\alpha)}{1-\alpha}\left[\theta_{n}^{m}-E_{\alpha}(-\mu_{\alpha}t_{n}^{\alpha})\theta_{0}^{m}\right]-\sum_{k=0}^{n-1}\left(A_{k}^{n}\theta_{k-1}^{m}+B_{k}^{n}\theta_{k}^{m}+C_{k}^{n}\theta_{k+1}^{m}\right)$$

$$=-\xi_{1}\left(\frac{(Q)_{n}^{m+1}-(Q)_{n}^{m-1}}{2h}-Q_{n}^{m}\frac{(Q)_{n}^{m+1}-(Q)_{n}^{m-1}}{2h}-\xi(Q_{n}^{m})^{2}\right)+R_{n}^{m},$$

$$[1+(1+\mu_{1})\theta_{n}^{m}+\mu_{2}Q_{n}^{m}]\frac{W(\alpha)}{1-\alpha}\left[Q_{n}^{m}-E_{\alpha}(-\mu_{\alpha}t_{n}^{\alpha})Q_{0}^{m}\right]-\sum_{k=0}^{n-1}\left(A_{k}^{n}Q_{k-1}^{m}+B_{k}^{n}Q_{k}^{m}+C_{k}^{n}Q_{k+1}^{m}\right)$$

$$=-\frac{1}{\xi_{1}}\left(\xi Q_{n}^{m}+\frac{(\theta)_{n}^{m+1}-(\theta)_{n}^{m-1}}{2h}+\xi_{2}\theta_{n}^{m}\theta_{x}+\xi_{3}Q_{n}^{m}\frac{(\theta)_{n}^{m+1}-(\theta)_{n}^{m-1}}{2h}\right)+R_{n}^{m}.$$

$$(15)$$

where

$$\theta_n^0 = \begin{cases} \theta_0(1 - \cos n\tau), & \text{if } 0 \le n \le N+1, \\ 0, & \text{if } n > N+1. \end{cases}$$
 (16)

$$Q_n^0 = \begin{cases} Q_0(1 - \cos n\tau), & \text{if } 0 \le n \le N+1, \\ 0, & \text{if } n > N+1. \end{cases}$$
 (17)

$$\theta_0^m = Q_0^m = 0, \qquad 0 \le m \le M + 1.$$
 (18)

 R_n^m is the truncation error of our scheme.

The difference scheme that results if the truncation error is disregarded is as follows:

$$(1 + \theta_{n}^{m}) \frac{W(\alpha)}{1 - \alpha} \left[\theta_{n}^{m} - E_{\alpha}(-\mu_{\alpha}t_{n}^{\alpha})\theta_{0}^{m}\right] - \sum_{k=0}^{n-1} \left(A_{k}^{n}\theta_{k-1}^{m} + B_{k}^{n}\theta_{k}^{m} + C_{k}^{n}\theta_{k+1}^{m}\right)$$

$$= -\xi_{1} \left(\frac{(Q)_{n}^{m+1} - (Q)_{n}^{m-1}}{2h} - Q_{n}^{m} \frac{(Q)_{n}^{m+1} - (Q)_{n}^{m-1}}{2h} - \xi(Q_{n}^{m})^{2}\right) + R_{n}^{m},$$

$$[1 + (1 + \mu_{1})\theta_{n}^{m} + \mu_{2}Q_{n}^{m}] \frac{W(\alpha)}{1 - \alpha} \left[Q_{n}^{m} - E_{\alpha}(-\mu_{\alpha}t_{n}^{\alpha})Q_{0}^{m}\right] - \sum_{k=0}^{n-1} \left(A_{k}^{n}Q_{k-1}^{m} + B_{k}^{n}Q_{k}^{m} + C_{k}^{n}Q_{k+1}^{m}\right)$$

$$= -\frac{1}{\xi_{1}} \left(\xi Q_{n}^{m} + \frac{(\theta)_{n}^{m+1} - (\theta)_{n}^{m-1}}{2h} + \xi_{2}\theta_{n}^{m}\theta_{x} + \xi_{3}Q_{n}^{m} \frac{(\theta)_{n}^{m+1} - (\theta)_{n}^{m-1}}{2h}\right) + R_{n}^{m}.$$

$$(19)$$

The system that is obtained is a set of algebraic equations that is nonlinear of size (N+1)(M+1) equations, that Newton's iteration techniques will be used to solve numerically [8].

4.1 Algorithm

Algorithm 1 Algorithm for solving the system using central difference scheme and fractional derivatives

- 1: Step 1: Define variables and parameters
- 2: Define θ_{nm} , Q_{nm} as approximate solutions
- 3: Set constants: h, τ , $W(\alpha)$, A_n^k , B_n^k , C_n^k
- 4: Step 2: Discretize the grid
- 5: Define spatial points n and time steps m
- 6: Set boundary conditions
- 7: Step 3: Approximate spatial derivatives
- 8: Use central difference method:

$$(\theta_x)_{mn} = \frac{\theta_{m+1,n} - \theta_{m-1,n}}{2h},$$

$$(Q_x)_{mn} = \frac{Q_{m+1,n} - Q_{m-1,n}}{2h}.$$

9: Step 4: Approximate fractional derivative using MABC

$$({}_{0}^{MABC}D_{t}^{\alpha}\theta_{t})_{n}^{m} = W(\alpha)(1-\alpha)\theta_{n}^{m} - \sum_{k=0}^{n-1} \left(A_{n}^{k}\theta_{k}^{m-1} + B_{n}^{k}\theta_{k}^{m} + C_{n}^{k}\theta_{k}^{m+1}\right).$$

- 10: Step 5: Update time steps
- 11: Update θ_n^m and Q_n^m using time-stepping method
- 12: Step 6: Iterate over time and space
- 13: Apply boundary conditions and iterate
- 14: Step 7: Analyze results
- 15: Plot and analyze θ_n^m and Q_n^m
- 16: Step 8: Check convergence and stability
- 17: Refine grid and time steps

5 Stability Analysis

Theorem 5.1. The numerical scheme described by (19) is conditionally stable for $\alpha \in (0,1)$ when the time step τ satisfies certain CFL-type conditions.

Proof. The stability can be shown using von Neumann analysis combined with the properties of the Mittag-Leffler function in the MABC derivative approximation. The detailed proof follows similar arguments as in [8].

5.1 Von-Neumann stability analysis

We examine the stability of the proposed scheme using the Von-Neumann technique. Following [22], system of (7) and (8) can be linearized as,

$$\mathcal{A}_{0}^{MABC}D_{t}^{\alpha}\theta_{t} = -\xi_{1}Q_{x} + \xi_{1}\mathcal{B}(\theta_{x} + \xi Q), \tag{20}$$

$$\mathcal{C}_{0}^{MABC}D_{t}^{\alpha}Q_{t} = -\frac{1}{\xi_{1}}\mathcal{D}(\xi + \xi_{3}\theta_{x}) - \frac{1}{\xi_{1}}\mathcal{E}\theta_{x}, \tag{21}$$

where A, B, C, D, and E are constants. Ignoring $-\frac{1}{\xi_1}D\xi$, we obtain,

$$Y_1 {}_0^{MABC} D_t^{\alpha} X_t = Y_2 X_x + Y_3 X, \tag{22}$$

with matrix definitions:

$$X = \begin{pmatrix} \theta \\ Q \end{pmatrix}, \qquad Y_1 = \begin{pmatrix} \mathcal{A} & 0 \\ 0 & \mathcal{C} \end{pmatrix},$$
 (23)

$$Y_2 = \begin{pmatrix} \frac{\xi_1 \mathcal{B}}{\xi_3 + \mathcal{E}} & -\xi_1 \\ -\frac{\xi_3 + \mathcal{E}}{\xi_1} & 0 \end{pmatrix}, \quad Y_3 = \begin{pmatrix} 0 & 0 \\ \xi_1 \xi \mathcal{B} & 0 \end{pmatrix}^T.$$
 (24)

5.2 Discretized system

System (22) is written below using MABC derivative as,

$$Y_{1} \frac{W(\alpha)}{1-\alpha} \left[X_{m}^{n} - E_{\alpha}(-\mu_{\alpha}t_{n}^{\alpha})X_{m}^{0} \right] - \sum_{k=0}^{n-1} \left[A_{k}^{n}X_{m}^{k-1} + B_{k}^{n}X_{m}^{k} + C_{k}^{n}X_{m}^{k+1} \right]$$

$$= Y_{2} \frac{(X)_{m+1}^{n} - (X)_{m-1}^{n}}{2h} + Y_{3}X_{m}^{n}, \tag{25}$$

or

$$G_1 X_m^n - G_2 X_m^0 - G_3 \sum_{k=0}^{n-1} X_m^{k-1} - G_4 \sum_{k=0}^{n-1} X_m^k - G_5 \sum_{k=0}^{n-1} X_m^{k+1} - G_6 X_{m+1}^n - G_6 X_{m-1}^n = 0, \quad (26)$$

N. H. Sweilam et al.

where

$$G_{1} = Y_{1} \frac{W(\alpha)}{1 - \alpha} - Y_{3}, \qquad G_{2} = Y_{1} \frac{W(\alpha)}{1 - \alpha} E_{\alpha}(-\mu_{\alpha} t_{n}^{\alpha}), \qquad G_{3} = \sum_{k=0}^{n-1} A_{k}^{n},$$

$$G_{4} = \sum_{k=0}^{n-1} B_{k}^{n}, \qquad G_{5} = \sum_{k=0}^{n-1} C_{k}^{n}, \qquad G_{6} = \frac{Y_{2}}{2h}.$$

5.3 Stability condition

Assume that,

$$X_m^n = \lambda^n \gamma \exp^{imh\Xi}, \quad i = \sqrt{-1}, \quad \Xi \in \mathbb{R}, \quad \gamma \in \mathbb{R}^{2 \times 1}, \quad \lambda \in \mathbb{R}^{2 \times 2},$$

substitute in (26), then,

$$G_1 \lambda^n \gamma \exp^{imh\Xi} - G_2 \mathbf{I} \gamma \exp^{imh\Xi} - G_3 \sum_{k=0}^{n-1} \lambda^{k-1} \gamma \exp^{imh\Xi} - G_4 \sum_{k=0}^{n-1} \lambda^k \gamma \exp^{imh\Xi} - G_5 \sum_{k=0}^{n-1} \lambda^{k+1} \gamma \exp^{imh\Xi} - G_6 \lambda^n \gamma \exp^{ih(m+1)\Xi} - G_6 \lambda^n \gamma \exp^{ih(m-1)\Xi} = 0.$$

Hence,

$$G_{1}\lambda^{n} - G_{2}\mathbf{I} - G_{3}\sum_{k=0}^{n-1} \lambda^{k-1} - G_{4}\sum_{k=0}^{n-1} \lambda^{k} - G_{5}\sum_{k=0}^{n-1} \lambda^{k+1} - G_{6}\lambda^{n} \exp^{ih\Xi} - G_{6}\lambda^{n} \exp^{-ih\Xi} = 0, \quad (27)$$

$$\sum_{k=0}^{n-1} \lambda^{k} = (\mathbf{I} - \lambda)^{-1} (\mathbf{I} - \lambda^{n}).$$

So,

$$G_1\lambda^n - G_2\mathbf{I} - G_3(\mathbf{I} - \lambda)^{-1}(\mathbf{I} - \lambda^{n-1}) - G_4(\mathbf{I} - \lambda)^{-1}(\mathbf{I} - \lambda^n) - G_5(\mathbf{I} - \lambda)^{-1}(\mathbf{I} - \lambda^{n+1}) - G_6\lambda^n \exp^{i\hbar\Xi} - G_6\lambda^n \exp^{-i\hbar\Xi} = 0.$$

We derive the stability condition,

$$|\lambda^{n}| = \left| \frac{G_{2}\mathbf{I} + G_{3}(\mathbf{I} - \lambda)^{-1}(\mathbf{I} - \lambda^{n-1})}{G_{1} - G_{6}(\exp^{ih\Xi} - \exp^{-ih\Xi})} + \frac{G_{4}(\mathbf{I} - \lambda)^{-1}(\mathbf{I} - \lambda^{n}) + G_{5}(\mathbf{I} - \lambda)^{-1}(\mathbf{I} - \lambda^{n+1})}{G_{1} - G_{6}(\exp^{ih\Xi} - \exp^{-ih\Xi})} \right| \le 1.$$

$$(28)$$

Theorem 5.2. The numerical scheme is stable when condition (28) is satisfied for all $\alpha \in (0,1)$ and appropriate time step τ .

Proof. The proof follows from Von-Neumann analysis and the properties of Mittag-Leffler functions, as detailed in [26].

6 Truncation Error Analysis

6.1 Error Estimation

The truncation error of our scheme is derived from,

$$(\theta_x)_n^m = \frac{\theta_n^{m+1} - \theta_n^{m-1}}{2h} + O(h^2), \tag{29}$$

$$(Q_x)_n^m = \frac{Q_n^{m+1} - Q_n^{m-1}}{2h} + O(h^2), \tag{30}$$

and the MABC derivative approximation,

$$(_{0}^{MABC}D_{t}^{\alpha}\theta_{t})_{n}^{m} = \frac{W(\alpha)}{1-\alpha} \left[\theta_{n}^{m} - E_{\alpha}(-\mu_{\alpha}t_{n}^{\alpha})\theta_{m}^{0}\right] - \sum_{k=0}^{n-1} \left[A_{k}^{n}\theta_{k-1}^{m} + B_{k}^{n}\theta_{k}^{m} + C_{k}^{n}\theta_{k+1}^{m}\right] + O(\tau^{4}),$$

$$(_{0}^{MABC}D_{t}^{\alpha}Q_{t})_{n}^{m} = \frac{W(\alpha)}{1-\alpha} \left[Q_{n}^{m} - E_{\alpha}(-\mu_{\alpha}t_{n}^{\alpha})Q_{0}^{m}\right] - \sum_{k=0}^{n-1} \left[A_{k}^{n}Q_{k-1}^{m} + B_{k}^{n}Q_{k}^{m} + C_{k}^{n}Q_{k+1}^{m}\right] + O(\tau^{4}).$$

Lemma 6.1. The overall truncation error of the scheme is,

$$R_n^m = O(\tau^4 + h^2). (31)$$

We conclude from the truncation error analysis that as the step size decreases in methods such as MABC, the accuracy of the approximation typically increases. However, the computational cost also increases with decreasing step size. To address this, one can compute the approximation error to determine an optimal value of h that balances computational efficiency and accuracy, enabling faster computations without compromising result quality.

7 Numerical Experiments

7.1 Implementation and results

This section presents numerical experiments to demonstrate the validity of the proposed method. Two numerical examples related to the stated problem are solved using the proposed approach. In addition, we analyze the effect of fractional differentiation on the behavior of the approximate solutions of the presented model. It is worth noting that all numerical computations are carried out using MATLAB R2023a.

Example 1: Let us take M=N=100, x=20, t=40, $\theta_0=1$, $Q_0=1$, $\xi=0.05$, $\xi_1=5$, $\xi_2=\xi_3=1.3$, $\mu_1=1,0.05$, $\mu_2=0$.

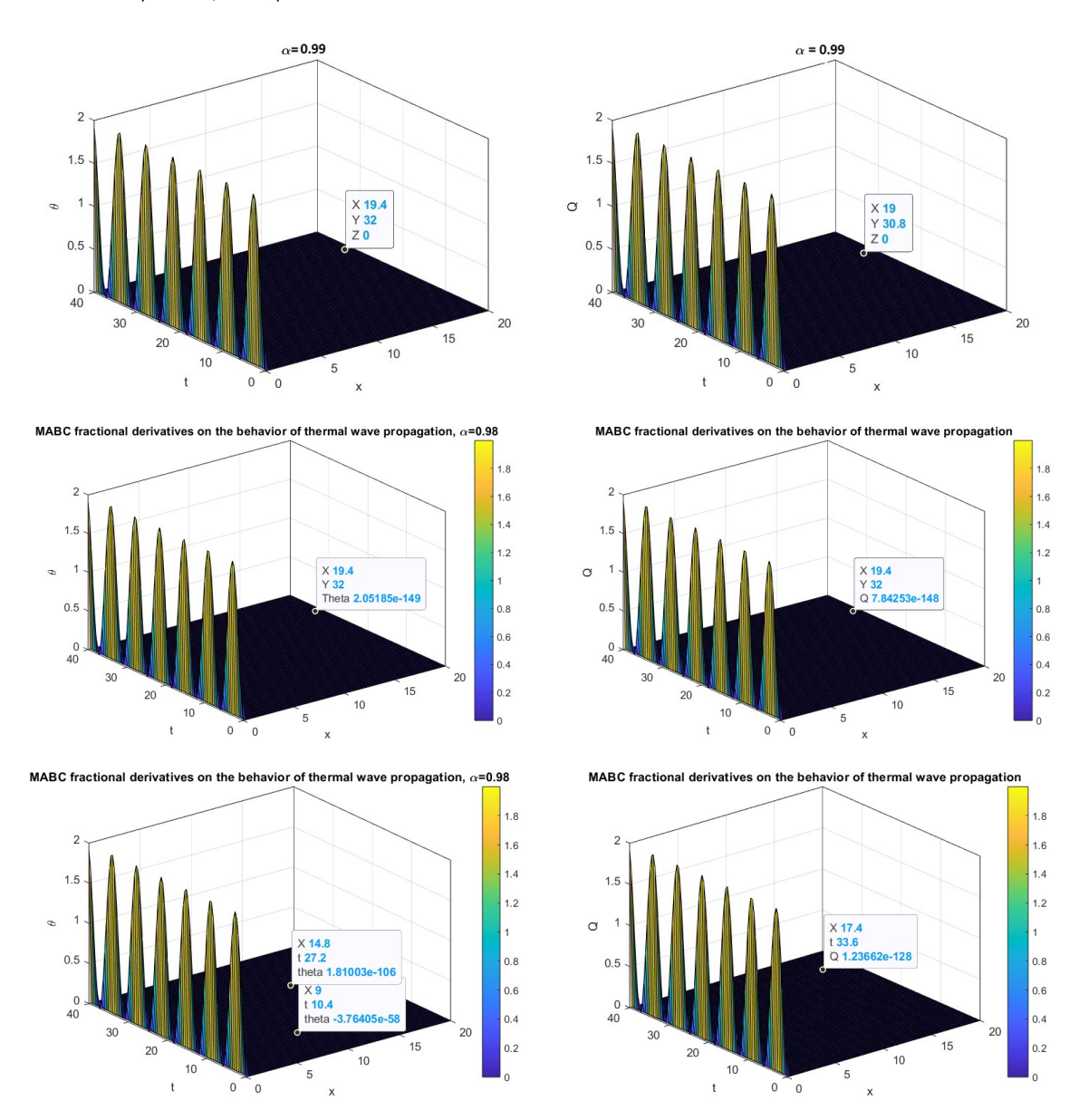


Figure 1: The solution's behavior for Example 1 at $\mu_1=1$.

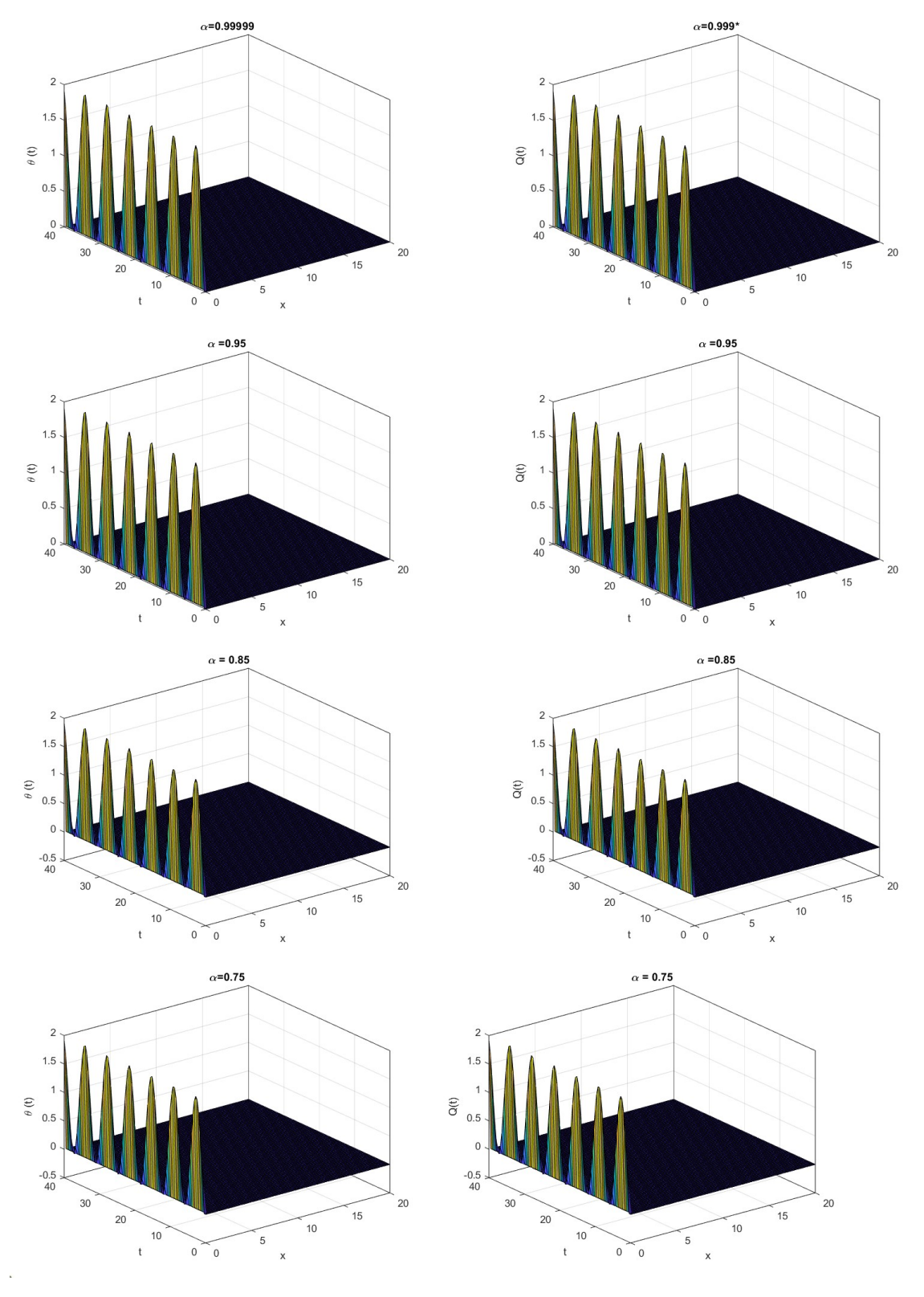
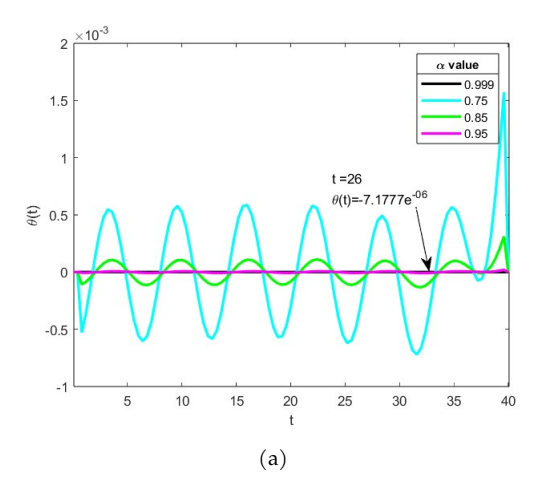


Figure 2: The solution's behavior for Example 1 at $\mu_1=0.05$.



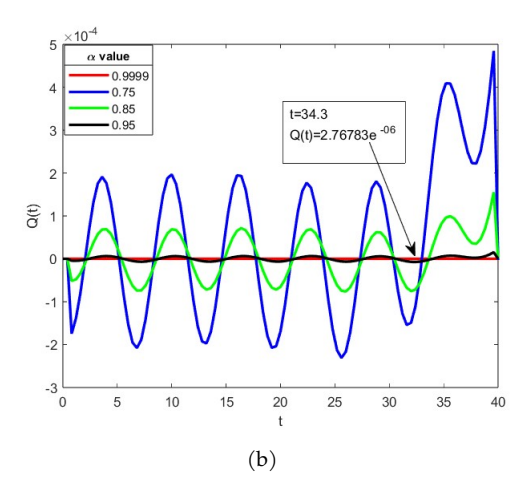


Figure 3: The solution's behavior for Example 1 at $\mu_1 = 0.05$.

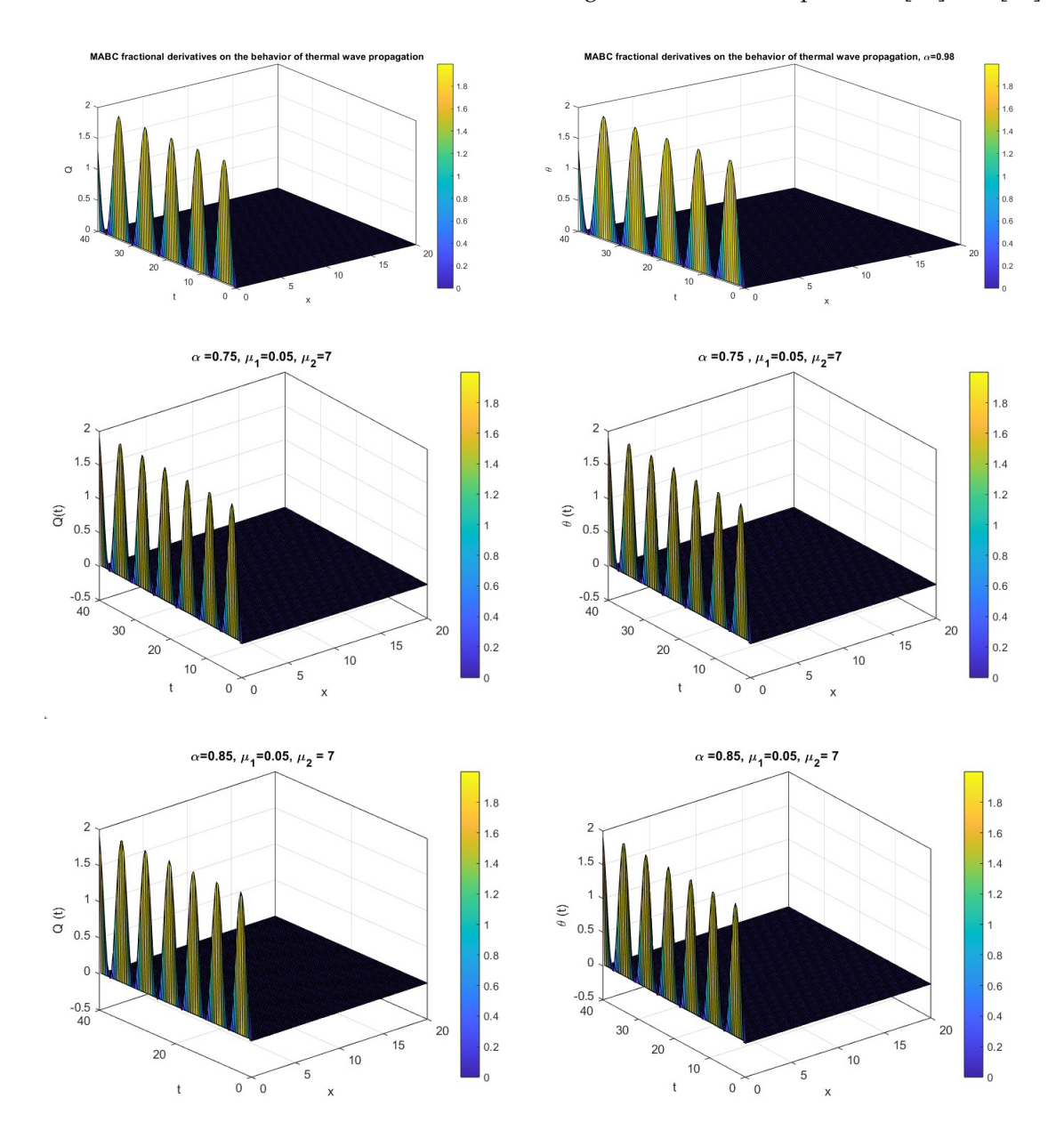
Figures 1 and 2 show the surface plots of the approximate solutions to examine the behavior of the obtained solution. These figures represent the solutions of Q and θ corresponding to $\mu_1=1$ and $\mu_1=0.05$, respectively. They illustrate the effects of the MABC derivatives of order α on the propagation of heat waves, which leads to memory-dependent thermal behavior and slower propagation. The frequency of the waves reflects nonlinear heat transfer dynamics and delayed thermal responses. Figure 2 illustrates the effect of the order α on the behavior of heat flow and temperature. The damped and repetitive appearance of the wave indicates that the fractional-order factor affects the heat transfer. The peaks of the graph indicate thermal pulses occurring at different times. The wave intensity decreases with increasing x, indicating a nonlinear propagation effect in the system. Figures 1 and 2 also show the influence of the parameter μ_1 on the propagation velocity of heat waves, revealing its subtle effect on the solution behavior.

Figure 3 presents two-dimensional graph showing the behavior of the solutions at different values of α . Figures 3(a) and 3(b) represent θ and Q solutions respectively corresponding to $\mu_1=0.05$. Figure 3(a) shows that lower values of α values (e.g., 0.75 in cyan) result in greater oscillatory activity and higher variations. Greater values of α (such as $\alpha=0.999$ in black) indicate a damped response with few oscillations. Similarly, Figure 3(b) exhibits increased oscillation amplitude and instability as α decrease (e.g., 0.75 shown in blue). Higher α values(e.g., 0.9999 shown in red) result in a more stable system with minimal oscillations. These results suggest that heat transfer becomes more unstable and oscillatory at lower fractional-order values (e.g., $\alpha=0.75$). The temperature profile is more steady and smooth with higher fractional-order values (e.g., $\alpha=0.9999$), suggesting classical-like behavior. This implies that unusual heat conduction processes, particularly in materials with memory-dependent characteristics, can be better captured by fractional derivatives.

Example 2: Let us take
$$M=N=100$$
, $x=20$, $t=40$, $\theta_0=1$, $Q_0=1$, $\xi=0.05$, $\xi_1=5$, $\xi_2=\xi_3=1.3$, $\mu_1=0.05$, $\mu_2=7$.

In this example, we study the effect of changing the parameter μ_2 at different values of α on the behavior of the solutions. The θ solutions are shown in the figures on the right, while the Q simulations are presented by the figures at the left. By comparing Figures

2 and 4, we observe that the effect of changing parameter μ_2 on the behavior of the solution is slight and almost negligible. The impact of order α on thermal conduction behavior and temperature is illustrated in Figure 4. Fractional heat equations provide a more accurate representation of the real thermal processes, which makes this study useful in material sciences, engineering, and thermal physics. Figure 4 indicates the temperature measurements and the occurrence of negative heat flux. These results are consistent with those obtained in the integer order cases, as reported in [28] and [27].



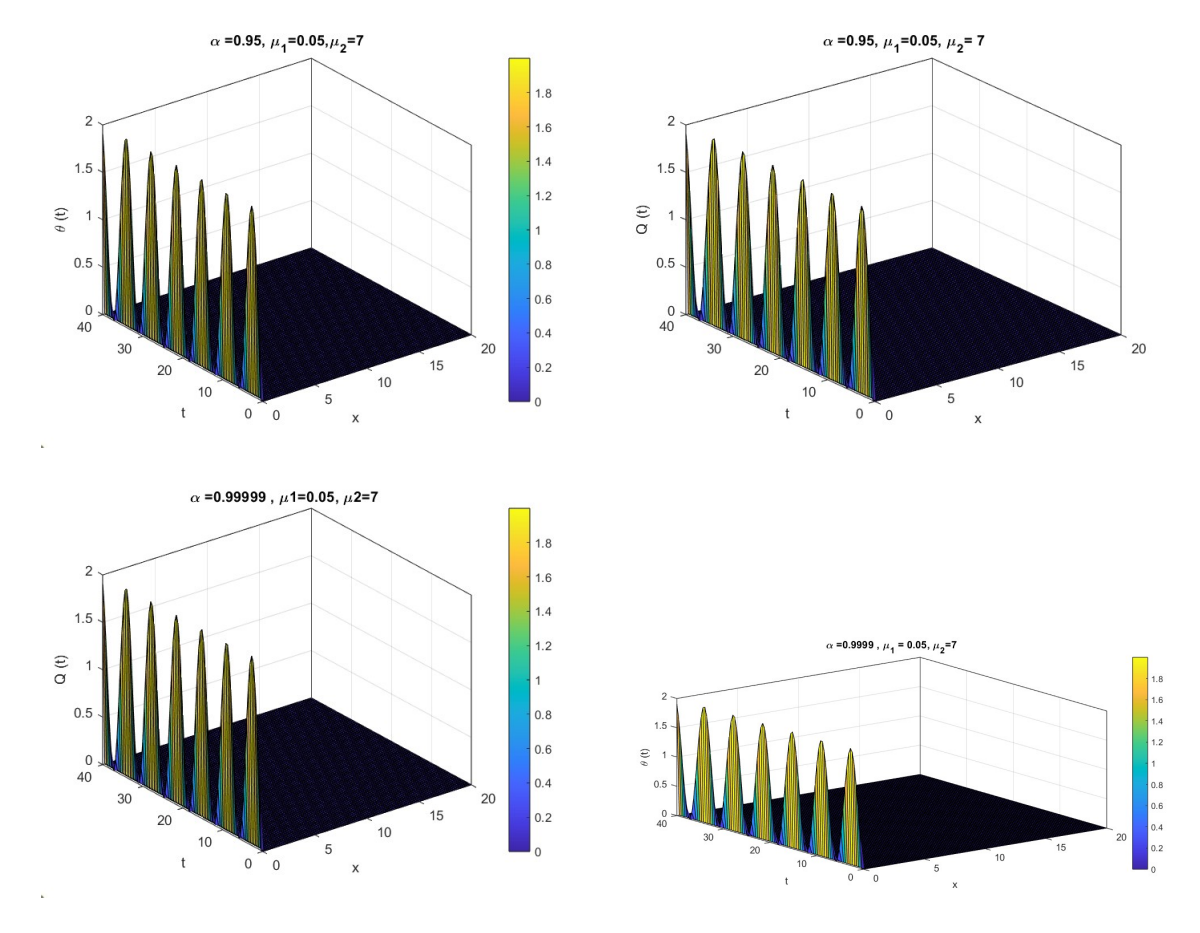


Figure 4: The solution's behavior for Example 2.

Figure 5 illustrates the influence of the fractional order α of the MABC derivative on the behavior of heat flow and temperature. Figures 5(a) and 5(c) show the solution behavior for Example 2 at various values of α , while Figures 5(b) and 5(d) present zoomed-in views of Figures 5(a) and 5(c), respectively. From these figures, we observe that smaller values of α lead to a more intense thermal response, indicating a stronger thermal memory effect. In contrast, larger values of α result in a slower and more stable response, suggesting that memory effects diminish over time. This leads us to conclude that the propagation of the thermal wave is influenced by the fractional order of the derivative, which reflects the conductive nature of the material. Thus, Figure 5 demonstrates how fractional coefficients affect the propagation of thermal waves in a nonlinear rigid conductor.

The order α of the MABC derivative has a considerable impact on the thermal response, as shown by the numerical simulations. Lower values of α indicate strong memory effects, producing pronounced thermal oscillations and delayed responses. In contrast, higher values of α lead to smoother, classical-like heat transfer, as memory effects become less significant. These results underscore the importance of selecting appropriate fractional orders when modeling heat transport in materials with memory-dependent behavior.

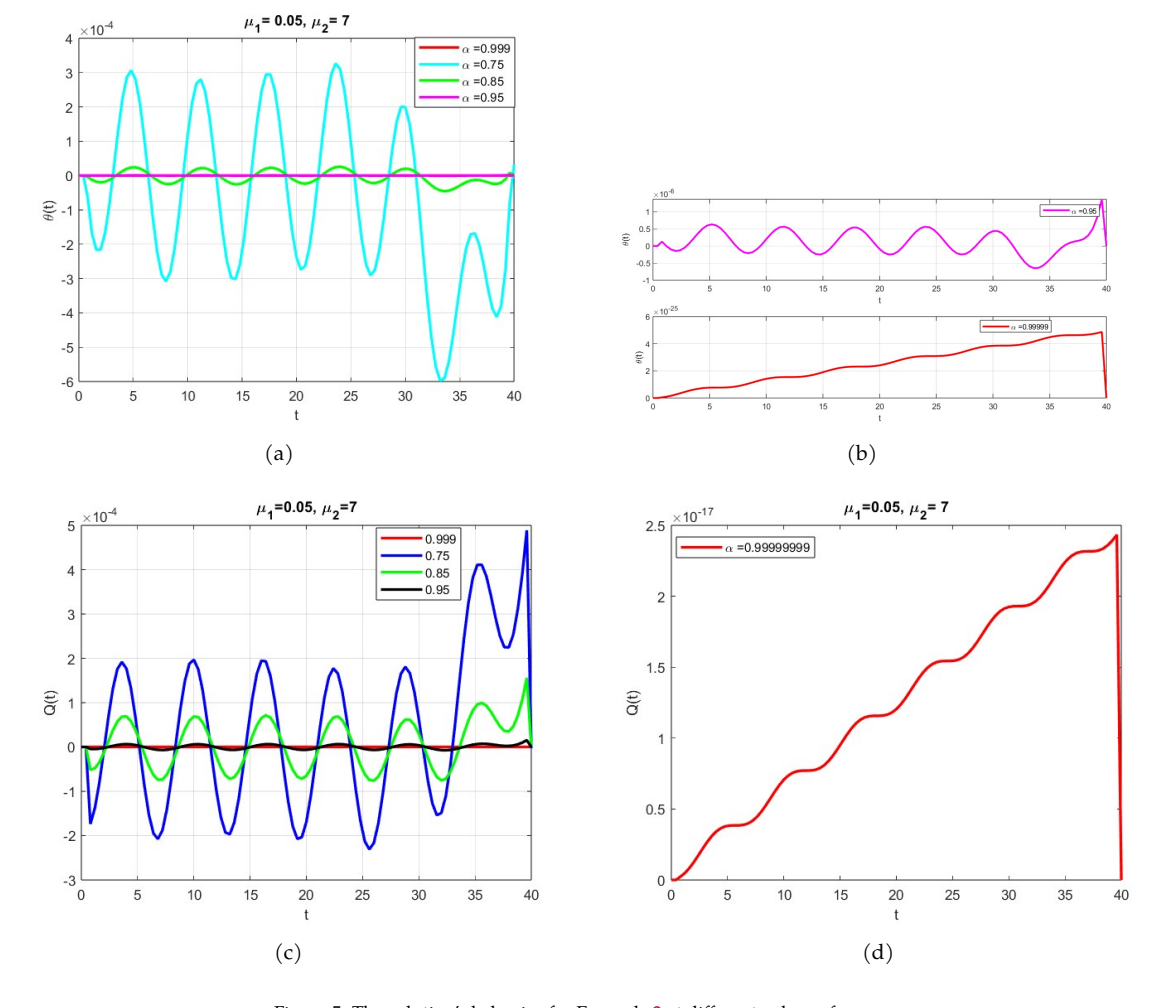


Figure 5: The solution's behavior for Example 2 at different values of α .

8 Conclusions

A dynamical model in the sense of MABC fractional derivative of dampened heat wave propagation was examined to predict the impact on heat flow and temperature in a stiff thermal conductive substance. A numerical technique with second-order spatial accuracy and fourth-order temporal accuracy is presented. Moreover, it is demonstrated that the numerical scheme is unconditionally stable using the Von-Neumann approach. Numerical experiments are displayed graphically to illustrate the obtained results.

Acknowledgement The authors would like to express their sincere gratitude to Prof. N. H. Sweilam and Dr. N. Bahaa El Din for their invaluable guidance, insightful discussions, and continuous support throughout the development of this research. Special thanks are also extended to Dr. M. K. Ammar and Prof. E. M. Abo-Eldahab for their valuable contributions to data preparation, software implementation and analysis. The collaborative effort among all authors has greatly enriched the quality and clarity of this work.

Conflicts of Interest On behalf of all authors, the corresponding author states that there is no conflict of interest

References

- [1] M. Abou-Dina, A. El Dhaba, A. Ghaleb & E. Rawy (2017). A model of nonlinear thermoelectroelasticity in extended thermodynamics. *International Journal of Engineering Science*, 119, 29–39. https://doi.org/10.1016/j.ijengsci.2017.06.010.
- [2] O. Abu Arqub, J. Singh & M. Alhodaly (2023). Adaptation of kernel functions-based approach with Atangana-Baleanu-Caputo distributed order derivative for solutions of fuzzy fractional Volterra and Fredholm integrodifferential equations. *Mathematical Methods in the Applied Sciences*, 46(7), 7807–7834. https://doi.org/10.1002/mma.7228.
- [3] M. Al-Refai & D. Baleanu (2022). On an extension of the operator with Mittag-Leffler kernel. *Fractals*, 30(05), Article ID: 2240129. https://doi.org/10.1142/S0218348X22401296.
- [4] A. Atangana (2016). New fractional derivatives with nonlocal and non-singular kernel: Theory and application to heat transfer model. *Thermal Science*, 20(2), 763–769. https://doi.org/10.2298/TSCI160111018A.
- [5] M. Caputo & M. Fabrizio (2015). A new definition of fractional derivative without singular kernel. *Progress in Fractional Differentiation & Applications*, 1(2), 73–85.
- [6] R. Chawla, K. Deswal, D. Kumar & D. Baleanu (2022). A novel finite difference based numerical approach for modified Atangana-Baleanu Caputo derivative. *AIMS Mathematics*, 7(9), 17252–17268. https://doi.org/10.3934/math.2022950.
- [7] I. C. Christov & P. Jordan (2010). On the propagation of second-sound in nonlinear media: Shock, acceleration and traveling wave results. *Journal of Thermal Stresses*, 33(12), 1109–1135. https://doi.org/10.1080/01495739.2010.517674.
- [8] B. P. Demidovich & I. A. Maron (1987). Computational Mathematics. Mir Publishers, Moscow.
- [9] S. Djennadi, N. Shawagfeh & O. A. Arqub (2020). Well-posedness of the inverse problem of time fractional heat equation in the sense of the Atangana-Baleanu fractional approach. *Alexandria Engineering Journal*, 59(4), 2261–2268. https://doi.org/10.1016/j.aej.2020.02.010.
- [10] J. Escolano, F. Rodríguez, M. Castro, F. Vives & J. A. Martín (2011). Exact and analytic-numerical solutions of bidimensional lagging models of heat conduction. *Mathematical and Computer Modelling*, 54(7-8), 1841–1845. https://doi.org/10.1016/j.mcm.2010.11.074.
- [11] K. M. Gaikwad & M. S. Chavan (2015). Vedic mathematics for digital signal processing operations: A review. *International Journal of Computer Applications*, 113(18), 10–14. https://doi.org/10.5120/19924-1503.
- [12] N. Hassan Sweilam & T. Abdulrahman Assiri (2015). Numerical scheme for solving the space-time variable order nonlinear fractional wave equation. *Progress in Fractional Differentiation & Applications*, 1(4), 269–280. https://doi.org/10.18576/pfda/010404.
- [13] P. Jordan (2015). Second-sound propagation in rigid, nonlinear conductors. *Mechanics Research Communications*, 68, 52–59. https://doi.org/10.1016/j.mechrescom.2015.04.005.

- [14] S. Julius, B. Leizeronok & B. Cukurel (2018). Nonhomogeneous dual-phase-lag heat conduction problem: Analytical solution and select case studies. *Journal of Heat Transfer*, 140(3), Article ID: 031301. https://doi.org/10.1115/1.4037775.
- [15] A. Khalouta & A. Kadem (2021). A new combination method for solving nonlinear Liouville-Caputo and Caputo-Fabrizio time-fractional Reaction-Diffusion-Convection equations. *Malaysian Journal of Mathematical Sciences*, 15(2), 199–215.
- [16] J. Li, Z. Fu, W. Chen & X. Liu (2019). A dual-level method of fundamental solutions in conjunction with kernel-independent fast multipole method for large-scale isotropic heat conduction problems. *Advances in Applied Mathematics and Mechanics*, 11(2), 501–517. https://doi.org/10.4208/aamm.OA-2018-0148.
- [17] B. Maayah, O. A. Arqub, S. Alnabulsi & H. Alsulami (2022). Numerical solutions and geometric attractors of a fractional model of the cancer-immune based on the Atangana-Baleanu-Caputo derivative and the reproducing kernel scheme. *Chinese Journal of Physics*, 80, 463–483. https://doi.org/10.1016/j.cjph.2022.10.002.
- [18] W. Mahmoud, G. Moatimid, A. Ghaleb & M. Abou-Dina (2020). Nonlinear heat wave propagation in a rigid thermal conductor. *Acta Mechanica*, 231, 1867–1886. https://doi.org/10.1007/s00707-020-02628-4.
- [19] S. A. Messaoudi & B. Said-Houari (2004). Blowup of solutions with positive energy in non-linear thermoelasticity with second sound. *Journal of Applied Mathematics*, 2004(3), 201–211. https://doi.org/10.1155/S1110757X04311022.
- [20] A. S. Moghadam, M. Arabameri, M. Barfeie & D. Baleanu (2020). Numerical solution of space-time variable fractional order advection-dispersion equation using Jacobi spectral collocation method. *Malaysian Journal of Mathematical Sciences*, 14(1), 139–168.
- [21] N. T. Phuong, N. T. Thanh Huyen, N. T. Huyen Thu, N. H. Sau & M. V. Thuan (2023). New criteria for dissipativity analysis of Caputo fractional-order neural networks with non-differentiable time-varying delays. *International Journal of Nonlinear Sciences and Numerical Simulation*, 24(7), 2649–2661. https://doi.org/10.1515/ijnsns-2021-0203.
- [22] R. Racke (2002). Thermoelasticity with second sound-exponential stability in linear and non-linear 1-d. *Mathematical Methods in the Applied Sciences*, 25(5), 409–441. https://doi.org/10.1002/mma.298.
- [23] P. Rogolino, R. Kovács, P. Ván & V. A. Cimmelli (2018). Generalized heat-transport equations: Parabolic and hyperbolic models. *Continuum Mechanics and Thermodynamics*, 30, 1245–1258. https://doi.org/10.1007/s00161-018-0643-9.
- [24] R. Saghatchi & J. Ghazanfarian (2015). A novel SPH method for the solution of dual-phase-lag model with temperature-jump boundary condition in nanoscale. *Applied Mathematical Modelling*, 39(3-4), 1063–1073. https://doi.org/10.1016/j.apm.2014.07.025.
- [25] N. H. Sau, N. T. Thanh, N. T. T. Huyen & M. V. Thuan (2022). Finite-time passivity for Atangana-Baleanu-Caputo fractional-order systems with nonlinear perturbations. *Circuits, Systems, and Signal Processing*, 41(12), 6774–6787. https://doi.org/10.1007/s00034-022-02135-y.
- [26] G. D. Smith (1985). *Numerical Solution of Partial Differential Equations: Finite Difference Methods*. Oxford University Press, Walton Street, Oxford.

- [27] N. Sweilam, M. Abou Hasan, S. Al-Mekhlafi & S. Alkhatib (2022). Time fractional of non-linear heat-wave propagation in a rigid thermal conductor: Numerical treatment. *Alexandria Engineering Journal*, 61(12), 10153–10159. https://doi.org/10.1016/j.aej.2022.03.034.
- [28] N. Sweilam, A. Ghaleb, M. Abou-Dina, M. A. Hasan, S. Al-Mekhlafi & E. Rawy (2022). Numerical solution to a one-dimensional nonlinear problem of heat wave propagation in a rigid thermal conducting slab. *Indian Journal of Physics*, *96*, 223–232. https://doi.org/10.1007/s12648-020-01952-8.